Environmental Pollution 393 (2026) 127517

Contents lists available at ScienceDirect

Environmental Pollution

journal homepage: www.elsevier.com/locate/envpol

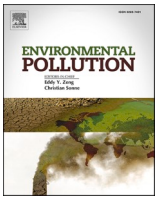

Legacy mercury emissions and releases from colonial-era gold mining in Australia☆

Larissa Schneider [a,*,1], Fei Cao [a,b,1,**], Peter Davies [c], Kathryn Allen [d], Simon Apte [a], James River Taylor [a], Quan Hua [e,f], Josh King [g], Ruoyu Sun [a,b], Matthew Theodore Brookhouse [h], Susan Lawrence [c]

[a] School of Culture, History and Language, The Australian National University, Coombs Bld. 9, Fellows Rd, Canberra, ACT, 0200, Australia
[b] Institute of Surface-Earth System Science, School of Earth System Science, Tianjin University, Tianjin, 300072, China
[c] Department of Archaeology and History, La Trobe University, Melbourne, Victoria, 3086, Australia
[d] School of Geography, Planning, and Spatial Sciences, University of Tasmania, TAS, 7005, Australia
[e] Australian Nuclear Science and Technology Organisation, Kirrawee DC, NSW, 2232, Australia
[f] School of Social Science, The University of Queensland, St. Lucia, QLD 4072, Australia
[g] CSIRO Environment, Bld. 135, Clunies Ross St, Acton, ACT, 2601, Australia
[h] Fenner School of Environment and Society, Australian National University, Forestry Building, 48 Linnaeus Way, Acton, 2601, Australia

A B S T R A C T

Legacy gold mining in Australia, closely tied to 19th-century colonisation and predating environmental protection laws, has left substantial mercury (Hg) contamination. Historical records in Walhalla, Victoria, indicate that Hg loss via the amalgamation process between 1867 and 1889 ranged between 2.65 tonnes and 34.4 tonnes, with further emissions in the following two decades. Dendrochemical analysis of exotic gymnosperms planted in Walhalla provides the first chronological record of colonial-era Hg emissions in Victoria. Local Bhutan cypress (*Cupressus torulosa*) and Douglas fir (*Pseudotsuga menziesii*) show elevated Hg during the peak of mining (1885–1914), reaching 44 ± 17 ng g^{-1} and 29 ± 9 ng g^{-1} respectively. Additionally, soils near gold-processing sites contain Hg at concentrations 2.5 orders of magnitude greater than background concentrations (41 ± 34 mg kg^{-1}). Stringers Creek sediments exceed the Australian high risk sediment guideline by 22 times (3.3 ± 3.4 mg kg^{-1}). Methylmercury (MeHg; 9.4 ± 10.8, max 32 ng g^{-1}) content of some waterfall sediments is in the global top 10 %. The nonlinear MeHg – total Hg relationship (Spearman $\rho = 0.93$, $p = 0.005$) suggests reduced methylation efficiency under high Hg loading. In soils, the relationship between total Hg vs. organic matter relation ($R^2 = 0.47$) indicates organic content is a driver of Hg retention. This study establishes an "emission–dendrochemistry–environment" evidence chain, confirming 19th-century mining as a major Australian Hg source with enduring ecological impacts and provides critical information that must be incorporated into national Hg management strategies.

1. Introduction

Mercury (Hg) is a potent neurotoxin that poses serious risks to human and ecological health, particularly through exposure to methylmercury (MeHg) in aquatic food webs (Basu et al., 2023). Although gold mining was historically one of the main sources of Hg release to the environment in Australia, the current extent, distribution, and persistence of this contamination remain poorly understood. Identifying where and at what levels Hg persists in the landscape is therefore critical for assessing ongoing environmental risks and informing management responses. While other studies in the Southern Hemisphere have demonstrated the hazards of Hg exposure associated with gold mining (e.g. Nyanza et al., 2025, 2020; Reuben et al., 2020), comparable data on contamination levels and potential exposure pathways in Australia are lacking (Fisher et al., 2023). Legacy gold mines in Australia are closely tied to colonisation during the 1800s. Mining operations at the time were not governed by environmental regulation and are believed to have released/emitted substantial quantities of Hg into soils, waterways and the atmosphere. While considerable attention has been given to Hg emissions and releases from legacy gold mines in the Americas (Cooke et al., 2009; Donovan et al., 2013; Eckley et al., 2020; Guerrero, 2017; Hohn et al., 2025), there has been far less focus on Australia, where

☆ This paper has been recommended for acceptance by Michael S. Bank.

* Corresponding author.
** Corresponding author. Institute of Surface-Earth System Science, School of Earth System Science, Tianjin University, Tianjin, 300072, China.
E-mail addresses: Larissa.Schneider@anu.edu.au (L. Schneider), caofei@tju.edu.cn (F. Cao).

[1] These authors contributed equally to this work.

https://doi.org/10.1016/j.envpol.2025.127517
Received 2 September 2025; Received in revised form 22 November 2025; Accepted 9 December 2025
Available online 11 December 2025

mining was also a central driver of the colonial economy and is likely to have been a significant contributor to global legacy Hg emissions.

Payable gold in Australia was first discovered in the colony of New South Wales in February 1851, followed by major discoveries further south in Victoria. Gold production from Victoria and New South Wales in the 1850s represented about 40 % of global output (Mudd et al., 2012). Over the next few decades, gold was discovered in Queensland (1860s), the Northern Territory (1870s) andWestern Australia (the Kimberley in the 1880s and the Coolgardie-Kalgoorlie field in the 1890s) (Blainey, 1963). In gold-rush regions, shallow alluvial mining was progressively replaced by the extraction of deeper hard-rock deposits undertaken by larger companies. Mercury-gold amalgamation was the main industrial process used for separating gold from the ore extracted from these latter sources (Birrell, 2004).

Legacy Hg from gold mining in Australia is not merely a historical issue. The chemical and physical properties of Hg mean that once released from geological reservoirs it can persist and recirculate across atmospheric, aquatic, and terrestrial systems for decades to centuries (Obrist et al., 2018). Therefore, the presence of Hg in the present-day environment is not solely driven by contemporary anthropogenic sources; it also reflects the continuing cycling of legacy emissions, including those from colonial-era gold-mining activities (Schneider and Guerrero, 2024). This ability to persist in the environment is particularly concerning in the case of MeHg. Methylmercury, the organic and most toxic form of Hg, readily bioaccumulates and biomagnifies in higher trophic level organisms. leading to elevated concentrations in predatory fish and humans. Once in the body, MeHg can cross both the blood–brain and placental barriers, impairing the neurological system in adults or disrupting normal foetal development (Aždajić et al., 2021).

The limited research on historical Hg releases in Australia means that the impact of colonial gold mining on local environments remains poorly understood, despite expectations (based on parallels with the Americas) that it may have been substantial. It also contributes to the lack of a national strategy for addressing Hg contamination at these legacy mine sites. The Australian Government's National Implementation Plan for the Minamata Convention, for example, does not acknowledge Hg pollution from historical mining activities, even though these sites likely represent one of the country's largest sources of historical Hg emissions (UNEP, 2025).

Given the limited data on historical Hg emissions from Australian legacy mines, there is a pressing need to characterise past atmospheric Hg levels. Palaeoecological archives, such as lake sediments and tree rings, offer promising avenues for reconstructing historical Hg emissions (Cooke et al., 2020). Water bodies across much of Australia, however, are limited, meaning that trees may be the more promising palaeo-archive for this kind of work. Where trees have clearly defined annual rings and elemental Hg taken up by the trees is not mobile across ring boundaries, they can provide a precisely dated history of past concentrations of atmospheric gaseous elemental Hg. Such trees therefore offer a means to better understand the long-term Hg emissions during colonial-era gold mining in Australia.

Annual rings are found in a range of Australian species, including the long-lived gymnosperms of Tasmania (La Marche et al., 1979; Ogden, 1978) and *Callitris* spp. in northern Australia (Allen et al., 2019; Baker et al., 2008). Annual rings are not, however, necessarily present in many of Australia's native and widespread species (Dunwiddie and LaMarche Jr, 1980; Gillen et al., 2021; Schweingruber, 1992). In many cases, whether bands are annual is not known because adequate testing has not been done. Additionally, long-lived gymnosperms, which are generally better Hg bioaccumulators than angiosperms (Gačnik and Gustin, 2023), are not commonly present across many areas where mining has occurred.

Walhalla, a small town located in west Gippsland in southern Victoria, was a geographically small but very rich goldfield. Two mines at Walhalla, the Long Tunnel and the Long Tunnel Extended, ranked as the first and fifth richest gold mines in Victoria respectively during the colonial mining period (Lloyd and Coombes, 2010; Swift and Marcuse, 1951). In addition to its exceptional gold production and Hg consumption, Hg emissions from mining activities in Walhalla are believed to have had a pronounced localised effect on the biogeochemical Hg cycle. This is attributed to the area's relatively high annual precipitation and its location within a steep, forested valley in the southern Great Dividing Range, which limits wind flow and promotes a wetter climate that enhances wet Hg deposition (via precipitation).

When the Walhalla township was established, the area was dominated by eucalypt forests. Within the township area, those forests were mostly cleared as Walhalla grew and mining activities expanded (Jenkins, 1998) and much of the surrounding vegetation is now predominantly composed of regrowth. While the native forests surrounding Walhalla are dominated by mixed stands of *Eucalyptus. dives*, *E. obliqua*, *E. cypellocarpa*, *E. sieberi* and *E. viminalis,* a suite of exotic tree species planted by early settlers are present in the township itself. Several of these exoctic trees are gymnosperms known to have annual rings in their region of origin (Butler, 2013).

This study aims to exploit the opportunity offered by tree rings, combined with documentary and sedimentary records, to examine Hg emissions at an annual scale in Walhalla. Specifically the study seeks to: (i) quantify the amount of Hg used at the Walhalla gold mine based on historical archival records; (ii) reconstruct historical Hg emissions during the gold mining boom (1864–1914) using dendrochemical analysis; (iii) assess current Hg concentrations in the main processing area of the Long Tunnel Mine; and (iv) evaluate the spatial distribution of Hg in Stringers Creek, the main watercourse of the area, through sediment sample analysis. By investigating the environmental effects of historical mining activities, this research will enhance our understanding of legacy pollution from colonial-era gold mining in Victoria. The findings emphasise the importance of more comprehensive assessments of Hg emissions and releases from colonial mines in Australia as a contributor to the Southern Hemisphere Hg cycle.

2. Methods

2.1. Physiography

The township of Walhalla is located on the southern slopes of the Great Dividing Range in eastern Victoria (latitude 37.9417° S, longitude 146.4486° E, c. 330m ASL). The township extends c. 2.5 km along a narrow mountain valley on both banks of Stringers Creek. The now heavily forested Stringers Creek is a sub-catchment of the Thomson River in West Gippsland and covers an area of c.19 km^2. The confluence of the left- and right-hand branches of Stringers Creek occurs in the Walhalla township (Fig. 1).

Walhalla's climate can be classified as cool-temperate. Mean monthly maximum temperatures range from just over 15 °C in April to 10.5 °C in September while minimum temperatures range from around 10 °C in February to 5 °C in September (Fig. S1) (Trewin, 2018). Rainfall is relatively evenly distributed throughout the year, but generally highest from August–November. Total annual rainfall averages just over 1100 mm (Fig. S1). The rainfall has weathered underlying tertiary sediments, resulting in leached colluvial soils that are moderately to strongly acidic. These soils are classified as Brown Dermosols (code DEAB) in the Australian Soil Classification (Isbel, 2021; Victorian Government, 2016). Dermosols in high rainfall areas such as Walhalla are usually moderately deep with a gradual increase of clay content with depth (McKenzie et al., 2004). Narrow alluvial terraces adjacent to the rocky beds of Stringers Creek support dark, organic-rich alluvial soils that are subject to frequent flooding.

The native vegetation around Walhalla can be characterised as damp sclerophyll forest, dominated by a tall eucalypt canopy at c.30 m over a medium dense shrub layer. Ground cover consists of herbs, grasses and ferns. Miners and residents at Walhalla also planted the township with an array of exotic northern-hemisphere angiosperm and gymnosperm

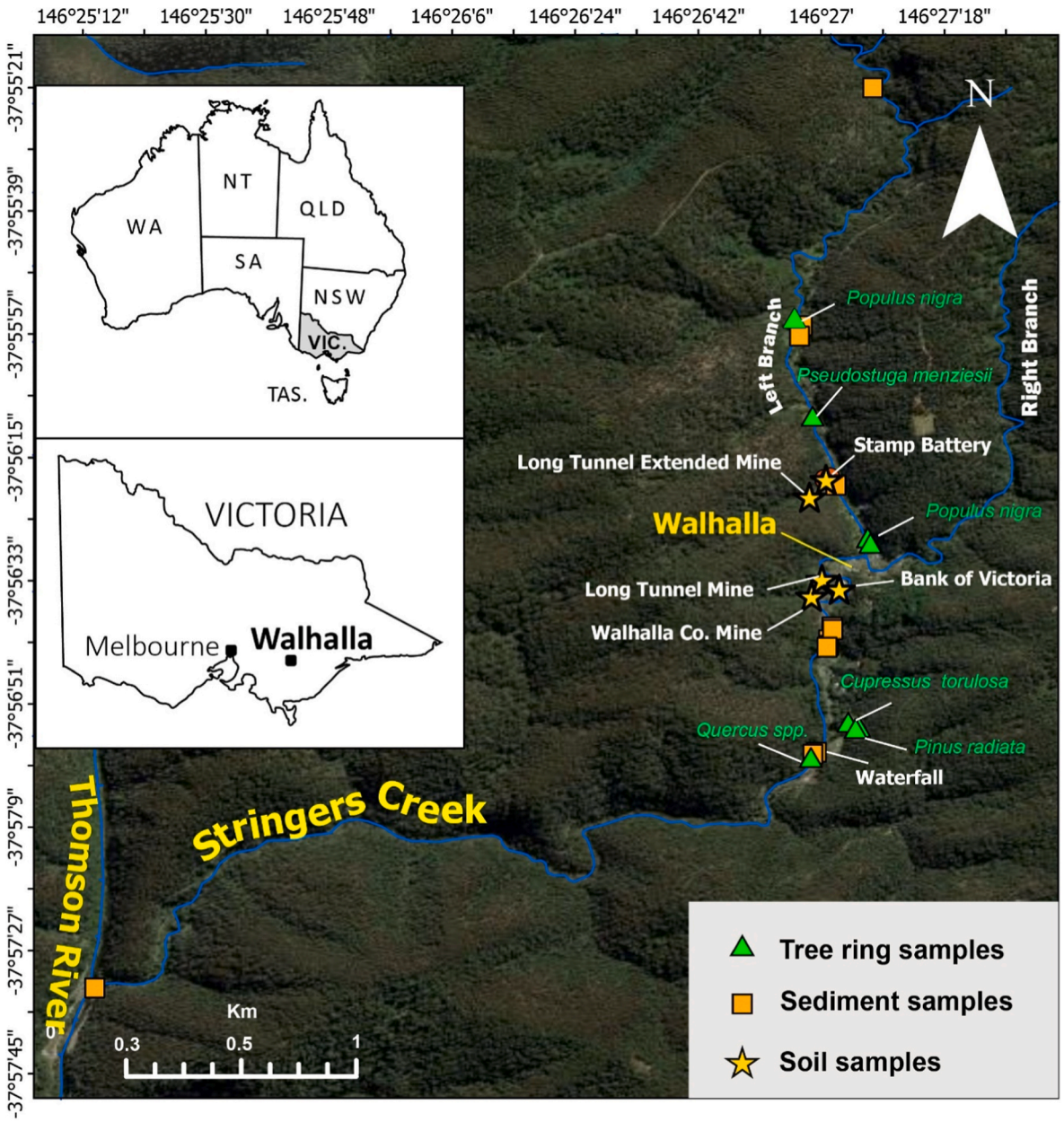

Fig. 1. Map of Walhalla, Victoria, showing the location of mining processing sites and location of tree ring, sediment and soil samples. Only oak (*Quercus* spp.), Douglas fir (*Pseudotsuga menziesii*), and Bhutan cypress (*Cupressus torulosa*) trees had growth rings spanning the mining period and were therefore analysed for total mercury.

taxa from the 1860s onward (Butler, 2013).

2.2. History

The gold rush in Victoria began in 1851, but it was not until January 1863, twelve years later, that alluvial gold was discovered at the remote site of Stringers Creek. Mining activity at Walhalla was primarily centred on extraction from Cohens Reef, located beneath the western hillside of Stringers Creek, within the Woods Point geological domain (Phillips et al., 2003). Cohens Reef comprises a north-south trending trough of compressed sedimentary strata, subsequently uplifted and deformed into a series of synclinal and anticlinal structures. Auriferous quartz veins formed at a later stage through hydrothermal injection along faults and fracture networks within the host sediments. Cohens Reef was the predominant auriferous quartz-carbonate vein system of the entire Gippsland goldfield. The main period of gold mining at Walhalla occurred between 1864 and 1914. Mining activity thereafter was negligible.

Dozens of gold mines operated within and around Walhalla over the years, but the region was dominated by three companies working adjacent claims along Cohens Reef: the Walhalla Company (1864–1881), the Long Tunnel Company (1864–1913), and the Long Tunnel Extended Company (1871–1911). The three companies produced, in total, more than 1.4 million troy ounces (~45 tonnes) of gold over a 49-year period, which was almost 2 % of all the gold mined in Victoria (Lloyd and Coombes, 2010).

By the early 20th century, gold yields had declined and most mines closed. Sawmilling and tourism gradually replaced goldmining as the main industries of Walhalla. Today, Walhalla is a heritage tourism destination, preserving remnants of its earlier mining past. Additional historical information, including details on ore crushing, Hg use, and smelting practices, is provided in the Supplementary Material.

2.3. Calculation of mercury loss during mining activities

Mining companies in Victoria used and discharged varying amounts of Hg during mineral processing during the gold rush (Mines Department of Victoria, 1868). Mercury was discharged and lost to the environment during mining mainly because the extraction and processing methods used were inefficient and lacked containment (Davies et al., 2015).

While historical records do not provide specific data on Hg acquisition and consumption for individual goldfields such as Walhalla, information on Hg losses to the environment during crushing and amalgamation at the Walhalla goldfield between 1867 and 1889 is available in the Mineral Statistics of Victoria (Victoria Department of Mines, 1890). We used these reports to estimate Hg lost to the environment at Walhalla from historical mining activity for the period 1867 to 1889. These records reported the number of stamp heads operating at each crushing battery and the corresponding range of Hg loss per stamp head per week. The published values are based on years of reporting by mine managers at Walhalla and are consistent with other mining areas across Victoria (Davies et al., 2015). At the time, quartz ore processing involved the addition of elemental Hg during crushing to form gold–mercury amalgams, followed by retorting to recover gold.

To estimate the range of Hg lost during mining activities, we multiplied the total number of stamp-heads by the minimum and maximum values of Hg lost per stamp head each week as reported in the Mineral Statistics of Victoria (Victoria Department of Mines, 1890). Our calculation assumed a working year of 40 weeks to allow for machinery breakdowns and other disruptions.

2.4. Collection of tree ring, soil and sediment samples

2.4.1. Tree rings

Core samples (a standard 5 mm diameter) were extracted from five exotic tree species in May (austral autumn) 2023. Two cores were obtained from each tree using a standard increment corer. These trees included one oak (*Quercus* spp.), one Douglas fir (*Pseudostuga menziesii*), five Lombardy poplar (*Populus nigra)*, one Monterey pine (*Pinus radiata)*, and five Bhutan cypress (*Cupressus torulosa)*.

The exotic trees analysed for total mercury (THg) in this study were assumed to be of similar age to one another and were planted by Walhalla residents during the mining boom. Tree locations are shown in Fig. 1. Tree cores were stored in plastic straws before being transported to the laboratory at the University of Tasmania where they were air dried and glued to wooden mounts.

2.4.2. Soil and sediment

Soil and Stringers creek sediment samples were collected during two field campaigns: the first in July 2022 (winter, labelled WAL0722) and the second in February 2023 (summer, labelled WAL0223). Sampling of soil was concentrated at the battery site of the Long Tunnel Extended Mine (Fig. 1), where historical documentation indicates that Hg was used in greatest quantities for gold amalgamation. The top 5 cm of soil was collected using a plastic hand trowel and stored in 50 mL plastic vials. This top 5 cm was assumed to represent current Hg concentration in the area with the highest likelihood of legacy contamination.

Sediment samples were collected along the length of Stringers Creek to enable spatial analysis of upstream and downstream Hg transport from the Long Tunnel Company and the Long Tunnel Extended Company mines (Fig. 1). Sampling in the lower reaches of the creek was limited due to difficult access associated with steep terrain and rocky surroundings. Samples were collected using a zinc-plated Petersen grab and stored in 50 mL high-density polyethylene centrifuge tubes (Falcon tubes; Thermo Fisher, Sydney, Australia). The sample volume of 50 mL was determined in accordance with the European Commission guidelines for trace metal analysis in sediment sampling (UNEP/MAP, 2019). To mitigate potential limitations associated with this relatively small volume, we collected field replicates at each site, sieved all samples to the <63 μm fraction to ensure compositional homogeneity, and performed analytical replicates on one-fifth of the samples to verify measurement precision.

Soil samples were collected from areas surrounding the ore-processing sites, where Hg was actively used. Sediment samples were collected along Stringers Creek, both upstream and downstream of the main processing site, to establish background concentrations, identify contaminated sections of creek, and assess the spatial distribution of Hg along the watercourse. All sediment samples were kept in a cooler with ice and transported to the Paleoworks Laboratory in the Department of Archaeology and Natural History, Australian National University, Canberra. Samples were kept frozen until freeze-dried.

2.5. Laboratory analyses

2.5.1. Tree ring count

Tree-ring cores were hand-sanded with successively finer grades of sandpaper until cellular detail in the wood was visible. Because all trees were alive at the time of coring in May 2023, the outermost ring was assumed to represent the 2022–2023 growing season. Cores within a single tree were visually crossdated and then measured using CooRecorder image analysis software. Visual crossdating involves matching of ring-width patterns and other features in the wood across samples from the same tree and then tree samples from the same species (where possible). In this study, crossdating among trees of the same species was only attempted for *Populus nigra* and *Cupressus torulosa*, as these were the only species for which multiple trees were sampled. Even for these species, however, very low sample numbers meant that achieving crossdating was difficult, particularly as the ring-width series were short (<150 years). We used the custom dendrochronological software, COFECHA, to statistically check the crossdating for these two species where possible (some of the *P. nigra* cores had too few rings for statistical crossdating).

Confirming the annularity or otherwise of ring counts in the sampled trees was crucial to being able to confidently determine a highly resolved Hg profile through time for the township. Uncertainty around the dates of wood, due to very low numbers of tree cores and consequently the inability to properly crossdate, meant we relied on Accelerator Mass Spectrometry radiocarbon (AMS ^{14}C) dating to validate ring counts for these cores.

2.5.2. Radiocarbon analyses of the tree cores

Prior to AMS dating, cores were sent to the Australian National University for THg analyses. Wood for THg analysis was extracted from the rings of the two cores of both *C. torulosa* and *Pseudotsuga menziesii* and one core of *Quercus* spp. These cores were chosen because they contained the longest ring-width series. For this analysis, it was assumed that rings were annual, a reasonable assumption based on previous work (Cufar et al., 2014; Freund et al., 2014; Fritts, 2001; Tshering et al., 2023; Watson and Luckman, 2002), although missing or false rings may distort ring counts.

There was no clear correspondence between the trend in time series of Hg in the *Quercus* spp. and the mining history based on ring counts. By contrast, both *C. torulosa* and *P. menziesii* contained trends in Hg that were consistent with Walhalla's mining history. Previous work has also suggested radial translocation may be an issue for *Quercus* spp (Gačnik and Gustin, 2023; Siwik et al., 2010). The *Quercus* spp. sample was consequently excluded from AMS ^{14}C dating and may therefore include some missing or false rings that could not be confirmed through a crossdating process because only a single oak in the township existed. Based on ring counts, tree-ring samples from Lombardy poplar (*Populus nigra*) and Monterey pine (*Pinus radiata*) did not extend back to the mining period (pre-1914) and were also excluded from both AMS ^{14}C dating and Hg analyses. This meas that for the analysis of THg concentration over time, a total of five tree cores was used: two from Bhutan

cypress (*C. torulosa*), two from Douglas fir (*Pseudotsuga menziesii*), and one from oak (*Quercus sp.)*.

One long tree core of *P. menziesii* (DF 1E), two long cores of *C. torulusa* (BT 1C, BT 2D), and one shorter core of *C. torulusa* (BT 5A) were sent to the Australian Nuclear Science and Technology Organisation (ANSTO) for AMS ^{14}C dating to validate ring counts (Supplementary Table S1). The shorter core was included as an additional test for annularity of rings in a structurally complex tree. A total of seventeen single rings were used for analysis. They included five rings each for cores BT 1C, BT 2D and DF 1E (three in the pre-1955 pre-bomb period, and two 1963–1968 — based on ring counts — in the bomb-peak period), and two rings for core BT 5A (in the bomb-peak period based on ring counts). For the two rings in core BT 5A, one ring in either side of the 1965 peak atmospheric bomb ^{14}C for the Southern Hemisphere (SH) zone 1–2 (Haines et al., 2018; Pearson et al., 2011; Witt et al., 2017) were analysed.

After being cut from the tree cores, the selected samples were washed in Milli-Q water in a sonic bath 3 times at 20 min each to remove water-soluble glue that held the tree cores to the wooden mounts. The samples were oven dried at 40 °C for 2 days and then sliced into thinner pieces along the growth axis of each ring using a surgical knife. Cellulose was then extracted from these samples (Němec et al., 2010) before being combusted and converted to graphite (Hua et al., 2001) for AMS ^{14}C measurements using the VEGA AMS facility (Wilcken et al., 2015) at ANSTO. The radiocarbon results were reported in percent modern carbon (pMC; Stuiver and Polach, 1977). Two approaches to obtain calendar ages (calibrated ages) for the measured pMC values were used. The first one was applied for the single ^{14}C values of the two youngest rings in each core by using CaliBomb program (Reimer et al., 2004) and bomb ^{14}C data for Southern Hemisphere (SH) zone 1–2 (Hua et al., 2022). The second approach employed wiggle matching of all five ^{14}C values in each of cores BT 1C, BT 2D and DF 1E using the D sequence (wiggle matching) in OxCal program v.4.4 (Bronk Ramsey, 2008). The radiocarbon calibration curve used for calendar age conversion in the second approach was the SHCal20 curve (Hogg et al., 2020), extended to the recent time using bomb ^{14}C data for SH zone 1–2 (Hua et al., 2022). All the radiocarbon results and their calibrated ages, and associated ring counts are presented in Supplementary Table S1.

2.5.3. Mercury analyses

All samples (soil, sediment and tree rings) were freeze-dried over 48 h using a Christ Alpha 1–2 LD plus lyophilizer prior to THg, MeHg and organic matter (OM) analyses. Following drying, soil and sediment samples were disaggregated and sieved to 63 μm using a stainless-steel laboratory sieve and a Fritsch Analysette Model 3 Spartan - vibratory sieve shaker. The <63 μm and >63 μm fractions were separated and stored individually. Only the <63 μm fractions were analysed for THg, MeHg and OM.

Soil, sediment and tree ring samples were analysed for THg using nickel boats and a Milestone Direct Mercury Analyser (DMA-80 Tricell; Milestone, Bergamo, Italy), following USEPA method 7473 (USEPA, 1998). The DMA-80 thermally decomposes all Hg species in solid samples to volatile Hg^0, which is preconcentrated using gold amalgamation and then quantified via atomic absorption spectrometry. To minimise instrumental bias and ensure comparability specifically for tree ring samples, all analyses were conducted using the same spectrometer cell 0, corresponding to the linear and most stable response range of the DMA detector.

Soil and sediment were analysed for THg in batches of 32 samples which also included two blanks and six reference material samples (Supplementary Table S2). Every fifth sample was run as a duplicate. The results of duplicate samples varied less than 10 % and are reported as mean concentrations. The standard reference material NIST 2706, New Jersey soil, from the National Institute of Standards and Technology USA, certified reference material from the National Water Research Institute (Environment Canada) WQB-1 (Lake Ontario) and the Joint Research Centre of the European Commission CC-141 (loam soil) were used for the THg analyses.

For tree-ring samples, P400-grade sandpaper was used to remove surface dust, followed by cleaning with compressed air. Rings were sectioned using a precision tree-ring cutter, which was thoroughly cleaned with ethanol and Milli-Q water between samples to minimise the risk of cross-contamination. Approximately 0.0150 g of wood (mean: 0.017 ± 0.015 g, n = 320) from each tree ring was loaded into nickel boats for THg analysis. For the interpretation of Hg emissions using tree rings, the mining period was defined as 1863–1914, corresponding to the years of active gold extraction and processing at the Walhalla site, including peak operations of the Long Tunnel Mine and the Long Tunnel Mine Extension Company. The post-mining period was defined as beginning in 1940, allowing a 26-year interval for atmospheric concentrations to return to background levels following the cessation of mining activities.

NIST standard reference materials 1515 (apple leaves) and NIST 1575a (pine needles) were used as reference materials for tree ring Hg analyses (Supplementary Table S2). A sample of NIST SRM 1515 was analysed after every 10 tree ring samples, and 1575a analysed after every 40 samples. The difference between the measured and certified Hg concentrations for the standard reference materials were less than 10 %. The mean concentrations of SRMs used to monitor and assess the stability of the DMA-80 were 44.8 ± 1.1 ng g^{-1} (n = 44, 1SD) and 39.4 ± 3.3 ng g^{-1} (n = 9, 1SD), with corresponding RSDs of 3 and 8 %, respectively, in agreement with the reported values (Supplementary Table S2).

Duplicate samples were run for every fifth sample. Results for these pairs varied less than 10 %. Where duplicates were taken, the results were averaged and the mean reported. For periods in which tree rings were too narrow to yield sufficient mass for Hg analysis, rings from adjacent years were combined to ensure Hg concentration could be accurately measured (Supplementary Table S3).

Methylmercury analysis on randomly selected sediment samples was carried out using a steam distillation/Gas Chromatography-Cold Vapour-Atomic Fluorescence Spectrometry (GC-CV-AFS) procedure based on the method developed by Bowles and Apte (2000). Up to 0.2 g of freeze-dried sediment was accurately weighed then placed in a glass distillation vessel, to which 10 mL of ultra-pure water and 2.5 mL distillation reagent (0.5 M $Cu(NO_3)_2$, 0.8 M KCl, 0.9 M H_2SO_4) was added. The vessel was placed into a heating mantle and ultra-pure steam passed through the solution, with distillate collected for 5 min. Sub-samples of distillate were diluted with ultra-pure water in amber glass vials and buffered to pH 4.9 with 2 M acetate buffer solution (and additions of 1 M KOH where required), to a final volume of approximately 40 mL. To this, 50 μL of a 2 % solution of sodium tetraethylborate was added and vials immediately capped, ensuring zero headspace, with Teflon-lined septa. MeHg concentrations were then quantified by GC-CV-AFS using an automated Merx-M instrument (Brooks Rand, Seattle, USA). Replicate distillations were carried out on 10 % of samples, with a relative standard deviation of 4 % achieved between replicates. Spike recovery of MeHg from spiked samples was 103 %. A portion of certified reference material DOLT-5 dogfish liver (National Research Council, Canada) was analysed in the sample batch to assess the extraction efficiency and accuracy of the combined distillation and analytical process, with a mean value of 131 ± 2 ng g^{-1} obtained (certified value 119 ± 58 ng g^{-1}).

2.5.4. Loss on ignition

Organic matter content in soil and sediment was estimated using loss-on-ignition (LOI) following the method described by Wang et al. (2011). Samples were dry-sieved to <63 μm, and approximately 1 g of each was placed in a muffle furnace (model CEMLL-SD; Labec, Sydney, Australia) and heated at 550 °C for 6 h. After cooling to room temperature, samples were reweighed, and the weight loss was calculated and reported as OM content in mass percentage (m/m).

2.6. Statistical analyses

All statistical analyses were conducted using R version 4.4.2 (R Core Team, 2025). Prior to analysis, THg, MeHg and OM concentrations were log-transformed to improve normality and reduce heteroscedasticity.

To evaluate differences in mean log-transformed Hg concentrations among tree species, a one-way analysis of variance (ANOVA) was performed. Tukey's Honest Significant Difference (HSD) post-hoc test was then applied to assess pairwise comparisons for significant Hg concentration differences.

Linear regression analysis was used to test for relationships between log-transformed total Hg concentrations and OM in soil and sediment samples. Additionally, Spearman rank correlation was applied to assess the relationship between MeHg and THg concentrations in stream sediments, given the non-linear nature of the association observed.

All statistical tests were two-tailed, and significance was assessed at the $\alpha = 0.05$ level. Figures and tables were generated using the base R plotting system and the ggplot2 package (Wickham et al., 2024).

3. Results and discussion

3.1. Historical mercury use and losses associated with gold mining in Walhalla

The historical records show that, despite recovery efforts to avoid Hg losses, significant Hg releases occurred through both tailings and atmospheric emissions during smelting (Birrell, 2004; Lloyd and Coombes, 2010). Typical crushing batteries contained five or more stamp heads and estimates of the range of Hg loss per stamp head were used to calculate total Hg losses over 23 years of operation, assuming a working year of 40 weeks. This relationship between stamp heads and Hg loss provides a quantitative basis for reconstructing the scale of historical Hg emissions at Walhalla, as larger crushing plants operating more stamp heads would have generated proportionally greater Hg discharges (James and Lee, 1970; Lerk, 2017).

Our analysis of historical records indicates that a minimum of 2.65 tonnes and a maximum of 34.4 tonnes of elemental Hg was lost to the environment at Walhalla due to quartz crushing and amalgamation over the 23-year period from 1867 to 1889 (Table 1). Mining companies at Walhalla continued to process auriferous quartz ores using Hg amalgamation for the following 20+ years, with gold production declining rapidly from 1914. Gold yields for the period 1890–1910 suggest that the total volume of Hg lost by amalgamation at Walhalla in these two decades was on a similar scale to the earlier period, which would include both elemental releases and atmospheric emissions.

Table 1
Estimated elemental mercury (Hg) loss at the Walhalla goldfield from 1867 to 1889, based on the number of operating stamp heads and reported weekly ranges of Hg loss. Calculations are based on the minimum and maximum values of elemental Hg lost per stamp head per week, multiplied by a working year of 40 weeks (data sources: Victoria 1852–1901, 1852).

Year	Stamp heads at Walhalla	Hg (oz) lost per stamp-head per week			Hg (kg) minimum loss in 40 weeks	Hg (kg) maximum loss in 40 weeks
1867	155	0.2	–	32	35	5625
1868	117	0.2	–	5	133	663
1869	112	0.5	–	5	64	635
1870	142	0	–	12	0	1932
1871	140	1	–	14	159	2223
1872	135	0.5	–	14	77	2143
1873	157	1	–	8	178	1424
1874	176	1	–	8	200	1597
1875	151	0.75	–	6	128	1027
1876	136	1	–	12	154	1851
1877	126	1	–	10	143	1429
1878	126	1	–	8	143	1143
1879	126	1	–	8	143	1143
1880	122	0.5	–	8	69	1107
1881	122	1	–	12	138	1660
1882	115	0.5	–	10	65	1304
1883	115	0.5	–	10	65	1304
1884	96	1	–	16	109	1742
1885	86	1	–	16	98	1560
1886	126	1	–	3	143	429
1887	136	1	–	4	154	617
1888	106	1	–	12	120	1442
1889	116	1	–	3	132	395
					2.65 kg	**34.4 kg**

3.2. Tree rings

Our tree ring series extended to 1885 (Supplementary Table S3). That span meant the first 20 years of mining (1864–1884) were not represented. A total of 320 tree rings from five cores (four trees) were analysed to reconstruct THg emissions over time (Supplementary Table S3).

3.2.1. Radiocarbon analyses and dendrochronology

The radiocarbon results were consistent with ring counts for four of the five cores tested (BT 1C, BT 2D, BT 5A and DF 1E) (Supplementary Table S1). This indicates the presence of annual rings in these cores. However, the AMS ^{14}C dating of core BT 5A indicated the presence of 6–9 false rings for the post-1964 period. Ring definition in this sample was poor at times, possibly partly due to the irregular trunk form and variable wood anatomy of *C. torulosa*. Additionally, the lack of longer series from the multiple trees of *C. torulosa* meant that crossdating—that would have helped identify these issues—was not possible. This discrepancy does not affect our analysis of THg concentrations during the mining period, however, as it pertains to the post-mining period, during which Hg concentrations show minimal interannual variation.

3.2.2. Post mining (background) species-specific differences in tree mercury concentrations

Comparison of THg concentrations between tree species was based solely on background levels (1940–2000), as the years in the mining period covered by different trees varied (Supplementary Table S3). Only a 10-year interval toward the end of the mining period was common to all species, limiting the ability to make consistent comparisons across the full mining timeline. Tree rings formed after 2000 were also excluded from the analysis, as this period lies outside the targeted period of the study. Moreover, recent rings are more susceptible to external damage or incomplete formation, which could introduce noise and bias into the dataset.

A one-way ANOVA indicated a statistically significant difference in mean log-transformed THg concentrations among species for the post-mining period ($F(2, 219) = 22.2$, $p < 0.001$). Post-hoc analysis using Tukey's HSD test revealed that mean log THg concentrations were significantly different between *Quercus* spp. (11.5 ± 3 ng g^{-1}) and *Pseudotsuga menziesii* ($\mu = 3.7 \pm 1.2$ ng g^{-1}) ($p < 0.001$), and between *Quercus spp.* and *C. torulosa* ($\mu = 4.7 \pm 1$ ng g^{-1}) ($p < 0.001$), but not between *P. menziesii* and *C. torulosa* ($p > 0.05$) (Fig. 2). These interspecific differences likely reflect variation in physiological traits and wood anatomy that influence Hg uptake, transport, and retention within the xylem. For example, differences in leaf morphology, transpiration rates, and the proportion of heartwood to sapwood can affect the relative contribution of atmospheric versus root Hg uptake and, consequently, Hg accumulation in tree rings (Liu et al., 2024). Environmental factors such as microclimatic conditions and soil Hg availability may further interact with these species-level traits, contributing to the observed variability (Obrist et al., 2012; Schneider et al., 2019; Siwik et al., 2010).

Background THg concentrations from the post-mining period (1940 onwards) in *P. menziesii* (mean 3.8 ng g^{-1}) and *C. torulosa* (mean 4.7 ng g^{-1}) are in the range of 3–5 ng g^{-1} (Table 2). These values fall within the

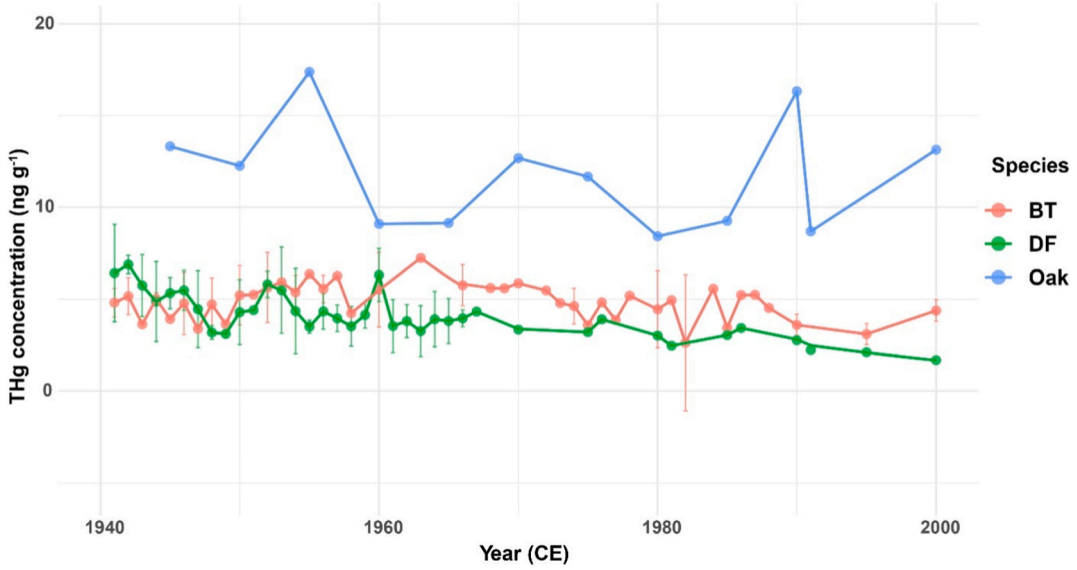

Fig. 2. Total mercury (THg) concentrations (ng g^{-1}) in tree cores from three species at the study site, covering the background period following mine closure (1940–2000) for interspecies comparison. Each line represents one species; for Bhutan cypress (*Cupressus torulosa*) (BT) and Douglas fir (*Pseudotsuga menziesii*) (DF). Error bars represent the variability across samples from the same tree. Note that the years assigned to oak rings are based solely on ring counts and not on radiocarbon (^{14}C) analysis. The figure was generated in R (version 4.4.2) using the ggplot2 and dplyr packages.

Table 2
Mean total mercury (THg) concentrations (ng g^{-1}) and standard deviations (SD) in tree rings from Walhalla, Victoria, Australia, during and post-mining periods.

		Bhutan cypress (*Cupressus torulosa*)		Douglas fir (*Pseudotsuga menziesii*)		Oak (*Quercus spp.*)
		BT1B	BT2D	DF1E	DF1B	OK
		ng g^{-1}		ng g^{-1}		ng g^{-1}
Post-mining (1940 to 2000)	**Average**	5.4	4.1	3.9	3.7	11.5
	SD	1.1	1.0	1.4	1.2	3.0
Mining (1885 to 1914)	**Average**	44	25	35	23	6.7
	SD	17	13	10	5.3	1.3
Fold increase		8.2	6.1	8.9	6.2	0.6

range of previously reported THg concentrations in tree rings, based on the literature (Gačnik and Gustin, 2023). *Pseudotsuga menziesii* tree rings from uncontaminated periods showed THg levels in the range of 2–5 ng g^{-1} near Seattle, Washington, USA (Obrist et al., 2012), in the Czech cities of Ústí and Labem (Boonen et al., 2025), and in Karlshausen in Germany (Land et al., 2025). No study was found on *C. torulosa* to allow direct comparison.

A notable finding in our study is that *Quercus spp.* exhibited higher THg concentrations than other species in the postmining period (Fig. 2). This corroborates findings from a recent systematic review of tree rings as archives of atmospheric Hg (Gačnik and Gustin, 2023), which consistently reported oak species (*Quercus spp.*) as not much less suitable for dendrochemistry studies than gymnosperms. The elevated Hg concentrations observed in oak rings during the post-mining period in our study are likely attributable to radial translocation, whereby Hg taken up by the tree during the mining period migrated into rings formed after mining had ceased. Radial translocation has previously been suspected in this species (Gačnik and Gustin, 2023; Siwik et al., 2010) and can result in homogenisation of Hg concentration gradients over time (Gačnik and Gustin, 2023; Liu et al., 2024; Siwik et al., 2010). Our results therefore add to the evidence that *Quercus spp.* is likely unsuitable for dendrochemical analysis.

3.2.3. Temporal record of mercury uptake in tree rings across mining and post-mining periods

The THg concentrations in the two other tree species tested reflects the historical pattern of gold mining activity in Walhalla (Fig. 3, Fig. 4), suggesting no or limited radial Hg translocation in either *C. torulosa* or *P. menziesii*. Although it was not possible to track THg concentrations throughout the entire operational period of the mine, the available results likely capture the period of THg emissions. This is supported by gold production records that show increase in Hg emissions corresponding to periods of peak gold output, followed by a sharp decline around 1914 as gold production decreased (Fig. 3).

A limitation of this study is the inability to collect tree-ring samples dating back to the onset of mining activities, owing to the absence of suitable native tree species for dendrochemical analysis. The appropriate exotic species were introduced only after the arrival of miners' families in the region (Butler, 2013), which constrained the temporal scope of sampling and prevented the reconstruction of contamination from the earliest phase of mining. The absence of gymnosperms suitable for dendrochemical analysis of Hg, in the surrounding native forests, further limits opportunities to extend the reconstruction.

The elevated Hg concentrations in tree rings from Walhalla during the mining period, approximately 7-fold above background concentrations (Fig. 4), is greater than that reported for other legacy gold-mining regions in Australia. For instance, in Tasmania, where colonial gold mining also occurred, Hg concentrations increased by only about 1.4-fold relative to background levels (Schneider et al., 2019). It also exceeds elevated levels observed in legacy gold mining sites in Canada (2.5-fold; Clackett et al., 2021) and California (around threefold; Wright et al., 2014). However, the during-mine enrichment in Walhalla remains lower than that reported for sites near historical Hg mines in Italy, where increases exceeded 20-fold (Baroni et al., 2023; Fornasaro et al., 2023).

3.3. Soil and sediment

The mean THg concentration in soils around the processing site of the Long Tunnel and Long Tunnel Extended mines was 41 ± 34 mg kg^{-1} (range: 2.2 – 95 mg kg^{-1}) (Fig. 5, Supplementary Table S5). Background soil Hg concentrations in the same region, in areas beyond the influence of mining activities, have been comprehensively characterised in a previous study (Taylor et al., 2025), which reported a mean

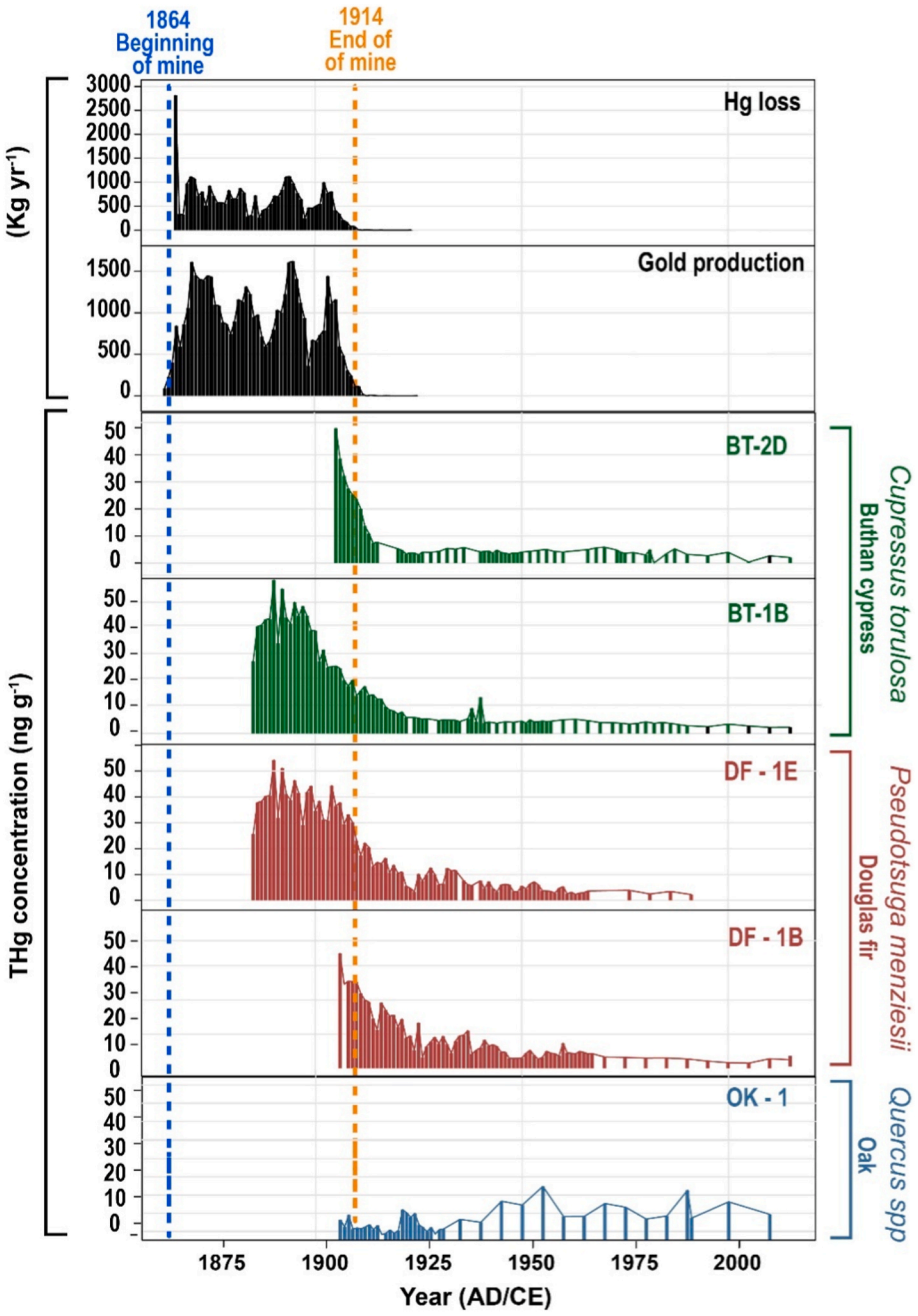

Fig. 3. Stratigraphic plots showing total mercury (THg) loss, gold production (kg yr^{-1}), and THg concentrations in tree rings of *Cupressus torulosa* (Bhutan cypress - BT), *Pseudotsuga menziesii* (Douglas fir - DF), and *Quercus spp*. (oak - OK) from Walhalla, Victoria. Note that some tree rings were combined to obtain sufficient mass for THg analysis. Oak ring years are based on ring counts only; other species use both ring counts and ^{14}C analysis. The plots were created in R (version 4.4.2) using the ggplot2, dplyr, and gridExtra packages. (For interpretation of the references to colour in this figure legend, the reader is referred to the Web version of this article.)

concentration of 0.112 ± 0.071 mg kg^{-1} in surface soils. The THg concentration measured in Walhalla soil is therefore approximately 2.5 orders of magnitude above these background concentrations.

For sediments, the mean THg concentration in samples collected along Stringers Creek, from upstream of the Long Tunnel and Long Tunnel Extended mines to its confluence with the Thompson River, was 3.3 ± 3.4 mg kg^{-1}, with concentrations ranging from 0.2 to 12 mg kg^{-1} (Fig. 5, Supplementary Table S5). The highest concentrations were found around the waterfall area with lower THg concentrations at the upper and downstream sites (Fig. 5).

Two samples, WAL 0722-1 and WAL 0722-3, were collected approximately 2 km upstream of the Long Tunnel and Long Tunnel Extended mines as an attempt to find background values (Fig. 5). However, their THg concentrations, 0.36 mg kg^{-1} and 0.20 mg kg^{-1} respectively, were higher than expected for the region based on previously reported regional average of 0.05 mg kg^{-1} for the Thompson River catchment (Schneider et al., 2021 and unpublished data).

Considering this regionally reported THg background in sediments, the average Hg concentration in Stringers Creek (3.3 mg kg^{-1}) was approximately 1.8 orders of magnitude higher than the regional background (average 0.05 mg kg^{-1}). When compared with the Australian sediment quality guidelines, all samples exceeded the default guideline value (DGV) of 150 ng g^{-1}. Furthermore, with the exception of eight samples located near the waterfall (Figs. 1 and 5), all others also

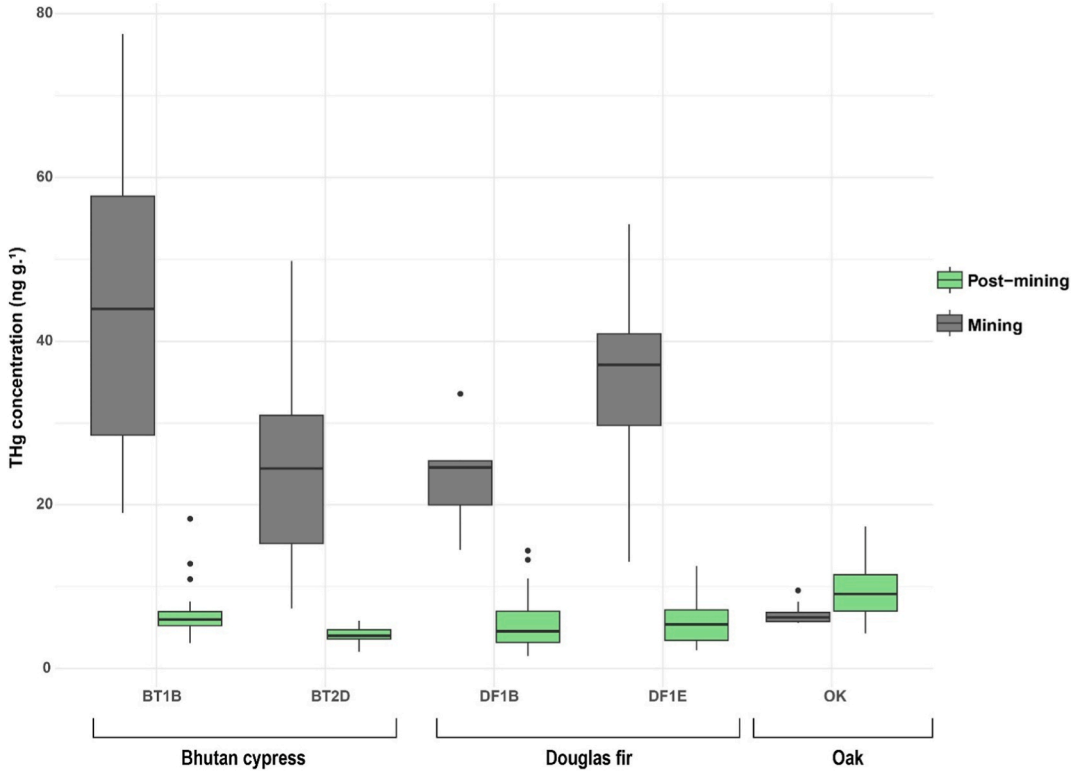

Fig. 4. Total mercury (THg) concentrations in tree rings of selected species from Walhalla, Victoria, comparing the mining and post-mining periods. The figure presents all measured values for during and post-mining periods. The figure was created in R (version 4.4.2) using the ggplot2 and dplyr packages.

exceeded the 'high' guideline value (GV-high) of 1000 ng g^{-1} which indicates a high probability of toxicity to sediment dwelling organisms (Australian Government, 2018).

Results from Walhalla soils and creek sediments show patterns comparable to those reported for legacy gold mines in California, USA. However, a fundamental difference lies in the gold extraction methods used. In California, miners employed hydraulic mining, which involved blasting hillsides with high-pressure water cannons to dislodge gold-bearing gravels (James et al., 2019; Kelley, 1954). This process generated large volumes of sediment, Hg used for amalgamation, and tailings that were washed directly into rivers, including the Yuba, Bear, Feather, and Sacramento Rivers (Nakamura et al., 2018; Singer et al., 2013).

In contrast to California, gold extraction in Walhalla was primarily from quartz reefs rather than alluvial deposits. Miners blasted quartz veins underground, hauled the ore to the surface, and crushed it in stamp batteries (Lawrence and Davies, 2020). Although the extraction processes differed from that in California, both locations shared a common outcome: the direct disposal of waste into waterways. In Walhalla, the steep topography of the valley left little space for tailings storage, leading miners to discharge tailings and other rejects directly into Stringers Creek (Lloyd and Coombes, 2010; Paull, 1963). In both the Californian and Australian cases, no containment or waste management practices existed at the time, and rivers themselves served as the primary disposal channels.

Over time, erosion of mine tailings and associated waste from historical mining areas has mobilised Hg downstream, where it accumulates in floodplains (Eckley et al., 2020; Holloway et al., 2009). In Walhalla, Hg concentrations in sediments from downstream sections of Stringers Creek, particularly near the waterfall, were higher than those near the mines (Fig. 5), indicating active erosion and sediment transport along the creek. Similar downstream enrichment patterns have been extensively documented in California. For instance, in the Cache Creek watershed of the Central California Coast Range, Hg concentrations in alluvial downstream sites along Bear Creek ranged from 0.5 to 10 mg kg^{-1}, while the main stem of Cache Creek ranged from 0.04 to 1.62 mg kg^{-1}, values comparable to those observed in Walhalla soils and sediments (Holloway et al., 2009).

Reworking of tailings has been a common feature of legacy mining sites, occurring both intentionally for additional gold recovery and passively through erosion, flooding, and human modification of waterways (Lawrence and Davies, 2014). This process is particularly important, as it can remobilise Hg long after mining activities have ceased, resulting in renewed contamination of surrounding environments.

At Walhalla, sediment loads in Stringers Creek increased markedly between 1863 and 1914, driven by mining disturbance, the production of mullock and tailings, and widespread vegetation clearance on surrounding slopes (James and Lee, 1970). From the 1880s, remnant tailings were reprocessed at several mills further downstream to recover fine residual gold (James and Lee, 1970). Major floods in 1891, 1934, 1952, 1978, 1990, and 2021 further mobilised large volumes of sediment and debris (SKM, 2006). In response, local residents and authorities realigned sections of the creek to reduce flood damage. Following the 1952 flood, the creek was cut westward through bedrock, forming the small waterfall and pool visible today (SKM, 2006).

Temporal sediment studies in the San Francisco Bay–Delta region demonstrate that peak Hg concentrations in sediment cores can occur nearly 50 years after the peak of mining activity (Conaway et al., 2004; Hornberger et al., 1999), indicating that sediments act as long-term Hg reservoirs that gradually release mercury through erosion and disturbance. A similar process is likely occurring in Walhalla. Our results show that Hg concentrations in the sedimentary record do not exhibit a simple downstream gradient from the processing site. Instead, the distribution reflects the influence of post-mining landscape processes (including erosion, sediment transport, and re-deposition) over more than a century. The principal hotspot of Hg accumulation occurs at the waterfall, representing a key area for targeted remediation (Fig. 5).

Mercury-contaminated sediments from Stringers Creek are transported into the Thomson River, which receives additional inputs from

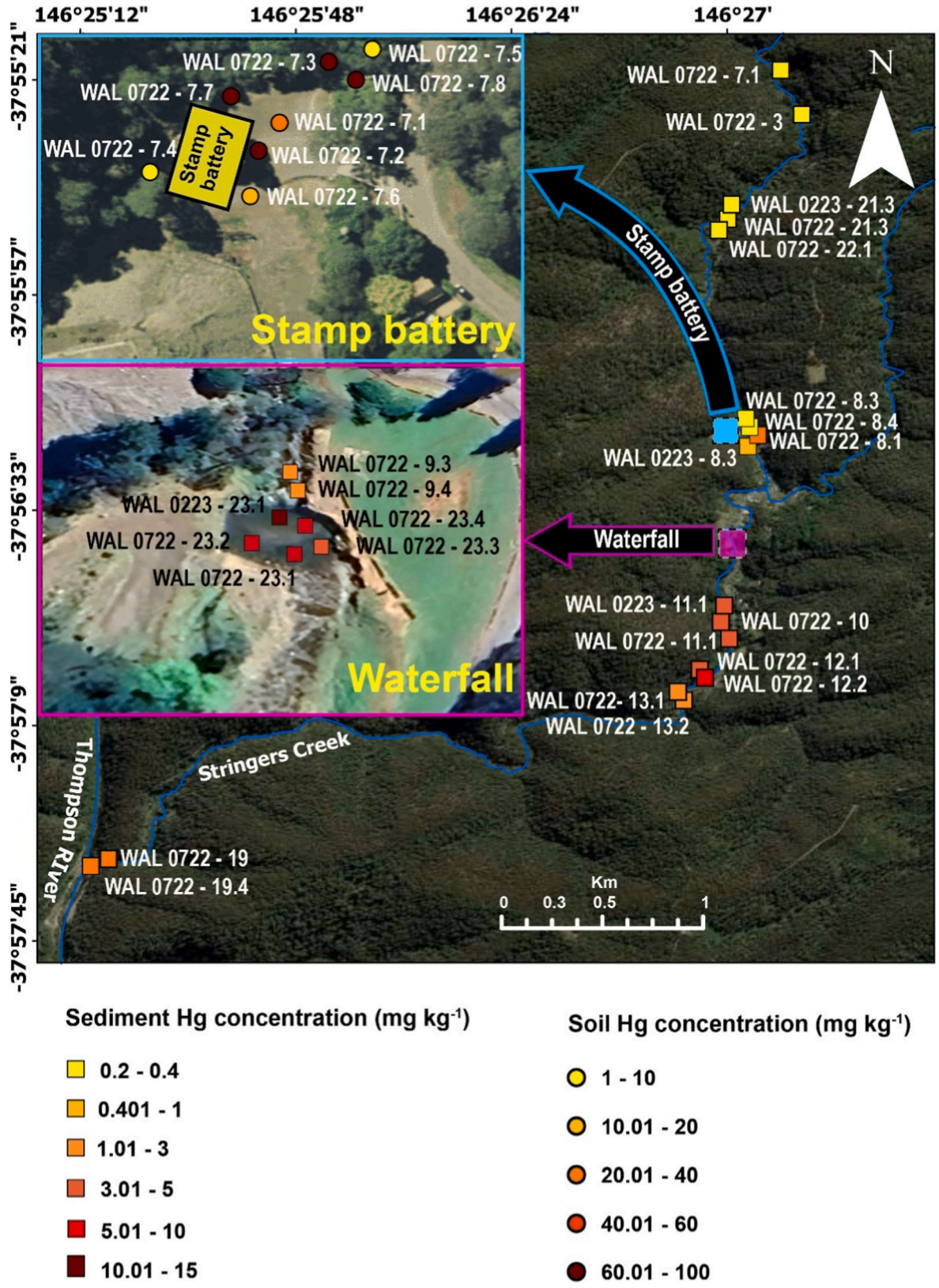

Fig. 5. Map of Walhalla, Victoria, showing the locations of soil and sediment sample sites. Total mercury (THg) concentrations (mg kg^{-1}) are represented using a gradient colour scale. Note that soil samples were collected exclusively from the historical ore processing site. Please refer to Supplementary Table S5 for absolute Hg concentration values. (For interpretation of the references to colour in this figure legend, the reader is referred to the Web version of this article.)

minor gold-mining tributaries. Approximately 90 km downstream, the Thomson River flows into the Gippsland Lakes, where extensive wetlands act as potential long-term sinks and secondary sources of legacy Hg. The Californian example, where peak Hg concentrations in sediments occurred decades after mining ceased, highlights the need for targeted studies in the Gippsland Lakes to determine whether they are accumulating Hg derived from Walhalla and other historical mining centres in the region.

3.3.1. Total mercury vs. organic matter

A significant positive relationship was observed between log total Hg concentration and log OM in soil ($R^2 = 0.47$, $p = 0.029$), while no significant relationship was found for sediment ($R^2 < 0.01$, $p = 0.905$) (Supplementary Fig. S3). The significant positive relationship in the soil likely reflects the higher OM of soils compared with sediments ($\mu = 27 \pm 9.3$ % and 3.3 ± 7.7 % respectively). Mercury has a strong affinity for organic compounds, and the greater abundance of OM in soils facilitates its binding and retention. In contrast, the sediments are relatively poor in organic matter, limiting Hg–OM interactions and resulting in the absence of a significant relationship. Therefore, OM plays a key role in retaining Hg within the soil matrix in Walhalla.

3.3.2. Methylmercury in sediments

Methylmercury (MeHg) concentrations in stream sediments collected from the six sampling locations are presented in Table 3. Concentrations ranged from 0.9 to 32.3 ng g^{-1}, with the highest values (19 and 32 ng g^{-1}) recorded at the waterfall area. Sites 8.3 and 23.1 were sampled in both summer (February 2022) and winter (July 2022). While the data suggest limited seasonal variation in MeHg concentrations at these locations (Table 3), further sampling is necessary to confirm this pattern with greater confidence.

To our knowledge, these values represent some of the highest MeHg concentrations reported in Hg-contaminated freshwater sediments globally. A comprehensive dataset was compiled by Cossa et al. (2014), comprising 1422 paired measurements of MeHg and THg in aquatic sediments. Comparison against this data set indicates that the two MeHg concentrations measured at the waterfall site fall above the 90th percentile of the global distribution. The highest sediment MeHg concentrations worldwide have generally been reported in Swedish riverine and estuarine environments heavily impacted by chlor-alkali activities (Drott et al., 2008; Paranjape and Hall, 2017). It remains unclear whether the waterfall area represents a localised hotspot for in situ Hg methylation, or a depositional zone for fine sediments enriched in MeHg produced elsewhere, such as through biomethylation within soils or tailings stockpiles.

A statistically significant positive relationship was observed between MeHg and THg in the stream sediments (Fig. 6, Spearman rank correlation: $\rho = 0.929$, $p = 0.005$). This relationship is consistent with the meta-analysis of global sediment Hg data reported by Cossa et al. (2014), which indicated a positive relationship between THg and MeHg in sediments. A global relationship between MeHg and total Hg concentrations in sediments ($n = 1442$) was identified, which followed a Michaelis-Menten-type curve. At low THg concentrations, MeHg levels increased proportionally with THg, indicating efficient methylation. However, at higher THg concentrations (>200 ng g^{-1}), MeHg production declined, suggesting a reduced methylation yield. This pattern was consistent across freshwater, estuarine, and marine sediment environments.

The proportion of MeHg relative to THg in the Stringer's Creek sediments ranged from 0.1 % to 1 % (Table 3), which falls within the typical range reported for aquatic sediments (Cossa et al., 2014). An inverse correlation between MeHg (%) and THg concentrations was observed (Supplementary Fig. S4), aligning with trends identified in the global dataset compiled by Cossa et al. (2014). Methylmercury concentrations in sediments and soils are governed by the balance between microbial methylation and demethylation processes, which occur simultaneously.

While THg concentrations are a key driver of MeHg production, the speciation of inorganic Hg also plays a critical role. In legacy mining environments, Hg was commonly introduced in its elemental form, either as vapour, liquid metal, or amalgam. Studies from historically Hg-contaminated sites, including former gold mining regions, have shown that elemental Hg is slow to oxidise and can persist in sediments for time periods of decades to centuries (NID, 2019). The slow oxidation of elemental Hg to form Hg^{2+} (Canela and Jardim, 1997; Gonzalez-Raymat et al., 2017) is likely to control the supply of Hg amenable to methylation, which is favoured by bacteria residing in low oxygen environments.

3.4. Mercury contamination in Walhalla: insights into Australia's contribution to the global mercury cycle

To our knowledge, this is the first study to investigate Hg in the Walhalla region. Previous research in Victoria focussed on Hg contamination has largely focused on surface waters and sediments downstream of former mine sites, including the Lerderderg River (Bycroft et al., 1982), Reedy Creek (Churchill et al., 2004), Raspberry Creek (Bos-VanderZalm, 2022), the Barwon Estuary (Reeves et al., 2015), and the Gippsland Lakes (Glover et al., 1980). Concentrations of Hg contained in sediments were above background (0.01–0.1 mg kg^{-1}), while water concentrations were generally at background levels for all these sites. The Melbourne and Metropolitan Board of Works (1975) recorded Hg at levels of 40–90 mg kg^{-1} Hg in soils near old mine batteries in the Thomson Valley. The Environment Protection Authority Victoria (EPAVIC, 2016) also found that 17 of 35 monitoring sites in ten historically mined rivers exceeded the sediment guideline of 0.15 mg kg^{-1}. They identified historical mines as the likely contamination source. To our knowledge, none of these studies assessed levels of MeHg present at the old mine sites or in rivers.

Although Walhalla is a regional case study, it reflects the broader legacy of colonial-era gold mining across Australia. During the nineteenth century, thousands of small- and medium-scale gold operations across Victoria and other states used Hg amalgamation methods similar to those at Walhalla (Lawrence and Davies, 2020). Collectively, the tree rings corresponding to the mining period, the soil samples collected near the battery, and the sediment samples from Stringers Creek where tailings were historically discharged, indicate that substantial quantities of Hg were emitted and released into the environment. Notably, these historical Hg releases to the Australian environment are largely absent from both national and global Hg inventories.

Australia currently does not prioritise Hg contamination from colonial mining within its environmental frameworks, including its obligations under the Minamata Convention (DCCEEW, 2024). This lack of recognition is significant, as colonial mining in the Southern Hemisphere likely represents one of the largest legacy sources of Hg to the hemispheric cycle.

Furthermore, Walhalla exemplifies the scale of emissions that have been overlooked in global models dominated by data from the Americas. Including Australian data is essential for accurately representing

Table 3
Concentrations of total mercury (THg) (mg kg^{-1}) and methylmercury (MeHg) (ng kg^{-1}) in stream sediment samples collected from Stringer's Creek catchment.

Sample ID	Date of collection	Season	THg (mg kg^{-1})	MeHg (ng g^{-1})	MeHg (%)
WAL0223–21.3	Feb-23	Summer	0.236	0.9	0.4
WAL0722–8.3	Jul-22	Winter	0.759	3.8	0.5
WAL0223–8.3	Feb-23	Summer	0.281	2.7	1.0
WAL0722–23.1	Jul-22	Winter	9.6	32.3	0.3
WAL0223–23.1	Feb-23	Summer	12.2	7.3	0.1
WAL0722–23.4	Jul-22	Winter	8.4	18.9	0.2
WAL0223–11.1	Jul-22	Winter	3.3	4.6	0.1
WAL0722–12.1	Jul-22	Winter	5.9	4.8	0.1

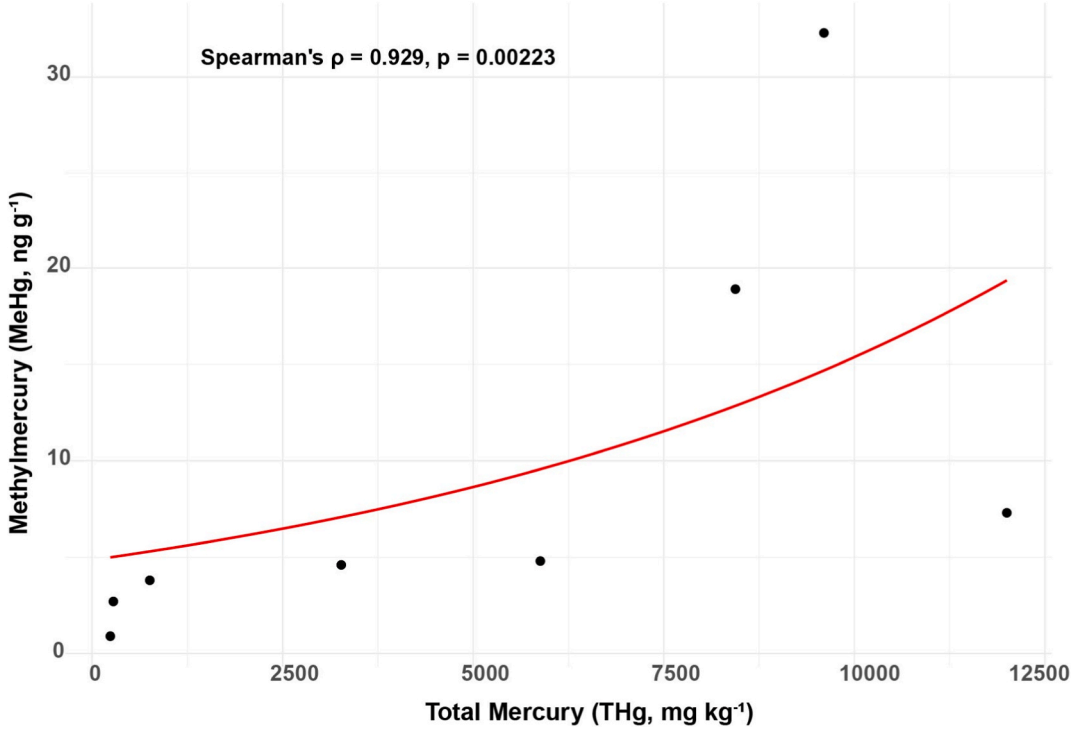

Fig. 6. Relationship between total mercury (THg) and methylmercury (MeHg) concentrations in sediment samples from Stringer's Creek. An exponential model of the form $MeHg = a \cdot e^{(b \cdot THg)}$ was fitted to the data. The red curve represents the fitted exponential regression. The figure was created in R (version 4.4.2) using ggplot2 and base stats/nls. (For interpretation of the references to colour in this figure legend, the reader is referred to the Web version of this article.)

historical and ongoing Hg fluxes. Without targeted remediation and monitoring, Hg exposure from contaminated sediments at Walhalla and other Victorian sites will persist for decades as the metal continues to be remobilised through local and downstream environments. Our findings show the need to incorporate colonial-era Hg pollution into both national management strategies and global assessments.

4. Conclusions

This study demonstrates that colonial-era gold mining at Walhalla has left a persistent legacy of Hg contamination in local soils and sediments. Mercury concentrations remain elevated more than a century after mining ceased, and methylmercury (MeHg) continues to form within contaminated sediments. The strong association between Hg and fine-grained material indicates that sediment mobilisation is the primary mechanism driving downstream Hg transport. The waterfall area was identified as a major hotspot for Hg accumulation and should be prioritised for remediation efforts.

Australia has had a significant history of Hg emissions, with Walhalla representing only one of many legacy mining sites that have contributed to long-term contamination. However, this history remains largely neglected in global Hg emission inventories and models, leading to an underestimation of the Southern Hemisphere's contribution to the global mercury cycle. These findings highlight the need for greater recognition of legacy Hg pollution from colonial-era mining in Australia and its integration into national environmental management and monitoring frameworks, consistent with the objectives of the Minamata Convention.

CRediT authorship contribution statement

Larissa Schneider: Writing – review & editing, Writing – original draft, Validation, Resources, Project administration, Methodology, Investigation, Funding acquisition, Formal analysis, Data curation, Conceptualization. **Fei Cao:** Writing – review & editing, Writing – original draft, Validation, Methodology, Formal analysis, Conceptualization. **Peter Davies:** Writing – review & editing, Writing – original draft, Visualization, Validation, Methodology, Investigation, Funding acquisition, Formal analysis, Data curation, Conceptualization. **Kathryn Allen:** Writing – review & editing, Writing – original draft, Visualization, Validation, Methodology, Formal analysis, Data curation, Conceptualization. **Simon Apte:** Writing – review & editing, Writing – original draft, Formal analysis. **James River Taylor:** Writing – review & editing, Formal analysis. **Quan Hua:** Writing – review & editing, Writing – original draft, Visualization, Validation, Methodology, Funding acquisition, Formal analysis, Data curation, Conceptualization. **Josh King:** Writing – review & editing, Formal analysis. **Ruoyu Sun:** Writing – review & editing, Writing – original draft, Formal analysis. **Matthew Theodore Brookhouse:** Writing – review & editing, Writing – original draft, Conceptualization. **Susan Lawrence:** Writing – review & editing, Writing – original draft, Methodology, Funding acquisition, Conceptualization.

Financial support

This study was funded by the Australian Research Council through the projects Lost Mines: The Troubled Legacies of Former Mining Landscapes (ARC DP220101967) and Long-range toxic metal pollution in Australia and the Southern Ocean (ARC DP220100828). Analysis of tree-ring ^{14}C by AMS was funded by ANSTO Research Portal Grant AP17652.

Declaration of competing interest

The authors declare that they have no known competing financial interests or personal relationships that could influence the work reported in this paper.

Acknowledgements

The authors acknowledge the Gunaikurnai people, the Traditional

Custodians of the land sampled for this study. The authors gratefully acknowledge John Rutter for his support during fieldwork.

Appendix A. Supplementary data

Supplementary data to this article can be found online at https://doi.org/10.1016/j.envpol.2025.127517.

Data availability

Data will be made available on request.

References

Allen, K.J., Brookhouse, M., French, B.J., Nichols, S.C., Dahl, B., Norrie, D., Prior, L.D., Palmer, J.G., Bowman, D.J.M.S., 2019. Two climate-sensitive tree-ring chronologies from Arnhem land, monsoonal Australia. Austral Ecol. 44, 581–596. https://doi.org/10.1111/aec.12699.

Australian Government, 2018. Sediment quality guideline values. Australian and New Zealand Guidelines for Fresh and Marine Water Quality. https://www.waterquality.gov.au/guidelines/anz-fresh-marine.

Ažđajić, M., Yumvihoze, E., Blais, J.M., Poulain, A.J., 2021. The effect of legacy gold mining on methylmercury cycling and microbial community structure in northern freshwater lakes. Environ. Sci. Process. Impacts 23, 1220–1230. https://doi.org/10.1039/D1EM00129A.

Baker, P.J., Palmer, J.G., D'Arrigo, R., 2008. The dendrochronology of Callitris intratropica in northern Australia: annual ring structure, chronology development and climate correlations. Aust. J. Bot. 56, 311. https://doi.org/10.1071/BT08040.

Baroni, D., Ancora, S., Franzaring, J., Loppi, S., Monaci, F., 2023. Tree-rings analysis to reconstruct atmospheric mercury contamination at a historical mining site. Front. Plant Sci. 14. https://doi.org/10.3389/fpls.2023.1260431.

Basu, N., Bastiansz, A., Dórea, J.G., Fujimura, M., Horvat, M., Shroff, E., Weihe, P., Zastenskaya, I., 2023. Our evolved understanding of the human health risks of mercury. Ambio 52, 877–896.

Birrell, R.W., 2004. The extraction of gold by amalgamation and chlorination. J. Australas. Min. Hist. 2, 17–34.

Blainey, G., 1963. The Rush that Never Ended: a History of Australian Mining. University Press, Melbourne.

Boonen, K., Shetti, R., Navrátil, T., Nováková, T., Jan, Rohovec, Lehejček, J., 2025. Atmospheric mercury pollution recorded in conifer tree rings: disentangling the effects of tree-ring width, water content, and climate on mercury concentrations. Dendrochronologia 92, 126370. https://doi.org/10.1016/j.dendro.2025.126370.

Bos-VanderZalm, C.H., 2022. Mercury in food web of Raspberry creek : an integrated report on mercury chemistry. Biology of Raspberry Creek. Monash University, Melbourne, VIC, Australia.

Bowles, K.C., Apte, S.C., 2000. Determination of methylmercury in sediments by steam distillation/aqueous-phase ethylation and atomic fluorescence spectrometry. Anal. Chim. Acta 419, 145–151.

Bronk Ramsey, C.B., 2008. Deposition models for chronological records. Quat. Sci. Rev., INTegration of Ice-core, Marine and Terrestrial records (INTIMATE): Refining the record of the Last Glacial-Interglacial. Transition 27, 42–60. https://doi.org/10.1016/j.quascirev.2007.01.019.

Butler, G., 2013. Walhalla Heritage Review 2013.

Bycroft, B.M., Coller, B.A.W., Deacon, G.B., Coleman, D.J., Lake, P.S., 1982. Mercury contamination of the Lerderberg River, Victoria, Australia, from an abandoned gold field. Environ. Pollut. Ser. A Ecol. Biol. 28, 135–147. https://doi.org/10.1016/0143-1471(82)90099-X.

Canela, M.C., Jardim, W.F., 1997. The fate of Hg0 in natural waters. J. Braz. Chem. Soc. 8, 421–423. https://doi.org/10.1590/S0103-50531997000400016.

Churchill, R.C., Meathrel, C.E., Suter, P.J., 2004. A retrospective assessment of gold mining in the Reedy Creek sub-catchment, northeast Victoria, Australia: residual mercury contamination 100 years later. Environ. Pollut. 132, 355–363. https://doi.org/10.1016/j.envpol.2004.03.001.

Clackett, S.P., Porter, T.J., Lehnherr, I., 2021. The tree-ring mercury record of Klondike gold mining at Bear Creek, central Yukon. Environ. Pollut. 268, 115777. https://doi.org/10.1016/j.envpol.2020.115777.

Conaway, C.H., Watson, E.B., Flanders, J.R., Flegal, A.R., 2004. Mercury deposition in a tidal marsh of south San Francisco Bay downstream of the historic New Almaden mining district, California. Mar. Chem., Special Issue in honor of Dr. William F. Fitzgerald 90, 175–184. https://doi.org/10.1016/j.marchem.2004.02.023.

Cooke, C.A., Balcom, P.H., Biester, H., Wolfe, A.P., 2009. Over three millennia of Mercury pollution in the Peruvian Andes. Proc. Natl. Acad. Sci. 106, 8830–8834. https://doi.org/10.1073/pnas.0900517106.

Cooke, C.A., Martínez-Cortizas, A., Bindler, R., Sexauer Gustin, M., 2020. Environmental archives of atmospheric Hg deposition – a review. Sci. Total Environ. 709, 134800. https://doi.org/10.1016/j.scitotenv.2019.134800.

Cossa, D., Garnier, C., Buscail, R., Elbaz-Poulichet, F., Mikac, N., Patel-Sorrentino, N., Tessier, E., Rigaud, S., Lenoble, V., Gobeil, C., 2014. A Michaelis–Menten type equation for describing methylmercury dependence on inorganic mercury in aquatic sediments. Biogeochemistry 119, 35–43. https://doi.org/10.1007/s10533-013-9924-3.

Cufar, K., Grabner, M., Morgós, A., Martínez del Castillo, E., Merela, M., de Luis, M., 2014. Common climatic signals affecting oak tree-ring growth in SE Central Europe. Trees (Berl.) 28, 1267–1277. https://doi.org/10.1007/s00468-013-0972-z.

Davies, P., Lawrence, S., Turnbull, J., 2015. Mercury use and loss from gold mining in nineteenth-century Victoria. Proc. Roy. Soc. Vic. 127, 44–54. https://doi.org/10.1071/rs15017.

DCCEEW, 2024. National Implementation Plan Minamata Convention on Mercury. Australian Government Department of Climate Change, Energy, the Environment and Water, Canberra, A.C.T. Australia.

Donovan, P.M., Blum, J.D., Yee, D., Gehrke, G.E., Singer, M.B., 2013. An isotopic record of mercury in San Francisco Bay sediment. Chem. Geol. 349–350, 87–98. https://doi.org/10.1016/j.chemgeo.2013.04.017.

Drott, A., Lambertsson, L., Björn, E., Skyllberg, U., 2008. Do potential methylation rates reflect accumulated methyl Mercury in contaminated sediments? Environ. Sci. Technol. 42, 153–158. https://doi.org/10.1021/es0715851.

Dunwiddie, P.W., LaMarche, Jr. V.C., 1980. Dendrochronological characteristics of some native Australian trees. Aust. For. 43, 124–135. https://doi.org/10.1080/00049158.1980.10674257.

Eckley, C.S., Gilmour, C.C., Janssen, S., Luxton, T.P., Randall, P.M., Whalin, L., Austin, C., 2020. The assessment and remediation of mercury contaminated sites: a review of current approaches. Sci. Total Environ. 707, 136031. https://doi.org/10.1016/j.scitotenv.2019.136031.

EPAVIC, 2016. Mercury and Arsenic in Victorian Waters: a Legacy of Historical Gold Mining. Environment Protection Authority Victoria, Melbourne. Report 1637.

Fisher, J.A., Schneider, L., Fostier, A.-H., Guerrero, S., Guimarães, J.R.D., Labuschagne, C., Leaner, J.J., Martin, L.G., Mason, R.P., Somerset, V., Walters, C., 2023. A synthesis of mercury research in the Southern Hemisphere, part 2: anthropogenic perturbations. Ambio 52, 918–937. https://doi.org/10.1007/s13280-023-01840-5.

Fornasaro, S., Ciani, F., Nannoni, A., Morelli, G., Rimondi, V., Lattanzi, P., Cocozza, C., Fioravanti, M., Costagliola, P., 2023. Tree rings record of long-term atmospheric Hg pollution in the Monte Amiata mining district (Central Italy): lessons from the past for a better future. Minerals 13, 688. https://doi.org/10.3390/min13050688.

Freund, J.A., Franklin, J.F., Larson, A.J., Lutz, J.A., 2014. Multi-decadal establishment for single-cohort Douglas-fir forests. Can. J. For. Res. 44, 1068–1078. https://doi.org/10.1139/cjfr-2013-0533.

Fritts, H.C., 2001. Tree Rings and Climate. The Blackburn Press, Caldwell, N.J.

Gačnik, J., Gustin, M.S., 2023. Tree rings as historical archives of atmospheric mercury: a critical review. Sci. Total Environ. 898, 165562. https://doi.org/10.1016/j.scitotenv.2023.165562.

Gillen, J., Costelloe, J., Allen, K., Fallon, S., Peel, M., M, S., Nathan, R., 2021. Can riparian eucalypts be used for hydroclimatic reconstruction? The case for Eucalyptus coolabah to define palaeo-flood events. J. Arid Environ. 184, 104301. https://doi.org/10.1016/j.jaridenv.2020.104301.

Glover, J.W., Bacher, G.J., Pearce, T.S., 1980. Gippsland Regional Environmental Study. Heavy Metals in Biota and Sediments of the Gippsland Lakes. Arthur Rylah Institute for Environmental Research, Melbourne., Melbourne, VIC, Australia.

Gonzalez-Raymat, H., Liu, G., Liriano, C., Li, Y., Yin, Y., Shi, J., Jiang, G., Cai, Y., 2017. Elemental mercury: its unique properties affect its behavior and fate in the environment. Environ. Pollut. 229, 69–86. https://doi.org/10.1016/j.envpol.2017.04.101.

Guerrero, S., 2017. Silver by fire, silver by Mercury: a chemical history of silver refining in new Spain and Mexico, 16th to 19th centuries. In: Silver by Fire, Silver by Mercury: a Chemical History of Silver Refining in New Spain and Mexico, 16th to 19th Centuries. Brill.

Haines, H.A., Olley, J.M., English, N.B., Hua, Q., 2018. Anomalous ring identification in two Australian subtropical *Araucariaceae* species permits annual ring dating and growth-climate relationship development. Dendrochronologia 49, 16–28. https://doi.org/10.1016/j.dendro.2018.02.008.

Hogg, A.G., Heaton, T.J., Hua, Q., Palmer, J.G., Turney, C.S., Southon, J., Bayliss, A., Blackwell, P.G., Boswijk, G., Ramsey, C.B., Pearson, C., Petchey, F., Reimer, P., Reimer, R., Wacker, L., 2020. SHCal20 Southern Hemisphere Calibration, 0–55,000 years cal BP. Radiocarbon 62, 759–778. https://doi.org/10.1017/RDC.2020.59.

Hohn, R.A., Abusaba, K.P., Bray, E.N., Hauswirth, S.C., Fuhrmann, B.C., Beutel, M.W., Lamborg, C.H., Mason, R.P., Flegal, A.R., Ganguli, P.M., 2025. Ongoing mercury contamination downstream from the former New Idria Mercury mine: southern diablo range of the California Coast ranges. PLOS Water 4, e0000328. https://doi.org/10.1371/journal.pwat.0000328.

Holloway, J.M., Goldhaber, M.B., Morrison, J.M., 2009. Geomorphic controls on Mercury accumulation in soils from a historically mined watershed, central California Coast Range, USA. Geochemical Studies of North American Soils: Results from the Pilot Study Phase of the North American Soil Geochemical Landscapes Project **24**. Appl. Geochem., pp. 1538–1548. https://doi.org/10.1016/j.apgeochem.2009.04.020

Hornberger, M.I., Luoma, S.N., van Geen, A., Fuller, C., Anima, R., 1999. Historical trends of metals in the sediments of San Francisco Bay, California. Mar. Chem. 64, 39–55. https://doi.org/10.1016/S0304-4203(98)80083-2.

Hua, Q., Jacobsen, G.E., Zoppi, U., Lawson, E.M., Williams, A.A., Smith, A.M., McGann, M.J., 2001. Progress in radiocarbon target preparation at the Antares AMS centre. Radiocarbon 43, 275–282. https://doi.org/10.1017/S003382220003811X.

Hua, Q., Turnbull, J.C., Santos, G.M., Rakowski, A.Z., Ancapichún, S., Pol-Holz, R.D., Hammer, S., Lehman, S.J., Levin, I., Miller, J.B., Palmer, J.G., Turney, C.S.M., 2022. Atmospheric radiocarbon for the period 1950–2019. Radiocarbon 64, 723–745. https://doi.org/10.1017/RDC.2021.95.

Isbel, R.F., 2021. The Australian Soil Classification: 4. CSIRO Publishing, Melbourne, VIC, Australia.

James, G.F., Lee, C.G., 1970. Walhalla Heyday. Robertson & Mullens, Melbourne, VIC, Australia.
James, L.A., Monohan, C., Ertis, B., 2019. Long-term hydraulic mining sediment budgets: connectivity as a management tool. Sci. Total Environ. 651, 2024–2035. https://doi.org/10.1016/j.scitotenv.2018.09.358.
Jenkins, T., 1998. Firewood Tramways of the Walhalla Mines 1865-1915 : a Research Paper on the History of the Firewood Tramways of the Walhalla Mines. Yarra Junction, Vic. : T & B J Publications.
Kelley, R.L., 1954. Forgotten giant: the hydraulic gold mining industry in California. Pac. Hist. Rev. 23, 343–356. https://doi.org/10.2307/3634653.
La Marche, V.C., Holmes, R.L., Dunwiddie, P.W., Drew, L.G., 1979. Tree-Ring Chronologies of the Southern Hemisphere. Laboratory of tree-ring Research. University of Arizona, Tucson, AZ - USA.
Land, A., Neugebauer, A., Franzaring, J., Schmidt, P., Biester, H., 2025. Global warming alters mercury accumulation in trees. EGUsphere 1–17. https://doi.org/10.5194/egusphere-2025-2325.
Lawrence, S., Davies, P., 2020. Historical mercury losses from the gold mines of Victoria, Australia. Elem. Sci. Anthr. 8, 35. https://doi.org/10.1525/elementa.432.
Lawrence, S., Davies, P., 2014. The Sludge Question: the Regulation of Mine Tailings in Nineteenth-Century Victoria. https://doi.org/10.3197/096734014X14031694156448 [WWW Document].
Lerk, J.A., 2017. On the Tail End. J.A. & E.R.S. Lerk, Bendigo., Bendigo, VIC, Australia.
Liu, X., Wang, X., Yuan, W., Wang, D., Feng, X., 2024. Tree rings recording historical atmospheric mercury: a review of progresses and challenges. Crit. Rev. Environ. Sci. Technol. 54, 445–462. https://doi.org/10.1080/10643389.2023.2250706.
Lloyd, B.E., Coombes, H., 2010. Gold in the Walhalla Region: West Gippsland. Victoria. Melbourne: Histec Publications., Melbourne, VIC, Australia.
McKenzie, N., Jacquier, D., Isbel, R.F., Brown, K.J., 2004. Australian Soils and Landscapes. CSIRO Publishing, Melbourne, VIC, Australia.
Melbourne and Metropolitan Board of Works, 1975. Report on Environmental Study into Thomson Dam and Associated Works. Volume 1. Melbourne and Metropolitan Board of Works, Melbourne. Melbourne, VIC, Australia.
Mines Department of Victoria, 1868. Mines department 1868. Mineral Statistics of Victoria. Mines Department, Melbourne.
Mudd, G.M., Giurco, D., Mohr, S., Mason, Leah, 2012. Gold resources and production: australia in a global context, CLUSTER RESEARCH REPORT no. 1.11. Prepared for CSIRO Minerals down Under Flagship, by the Department of Civil Engineering (Monash University) and the Institute for Sustainable Futures. University of Technology, Sydney). October 2012. ISBN978-1-922173-47-8.
Nakamura, T.K., Singer, M.B., Gabet, E.J., 2018. Remains of the 19th century: deep storage of contaminated hydraulic mining sediment along the lower yuba River, California. Elem. Sci. Anthr. 6, 70. https://doi.org/10.1525/elementa.333.
Němec, M., Wacker, L., Hajdas, I., Gäggeler, H., 2010. Alternative methods for cellulose preparation for AMS measurement. Radiocarbon 52, 1358–1370. https://doi.org/10.1017/S0033822200046440.
NID, 2019. Bear River Background. Nevada Irrigation District. Nevada Irrigation District (NID), San Francisco, USA.
Nyanza, E.C., Dewey, D., Manyama, M., Martin, J.W., Hatfield, J., Bernier, F.P., 2020. Maternal exposure to arsenic and mercury and associated risk of adverse birth outcomes in small-scale gold mining communities in Northern Tanzania. Environ. Int. 137, 105450. https://doi.org/10.1016/j.envint.2019.105450.
Nyanza, E.C., Mhana, R.J., Asori, M., Thomas, D.S.K., Kisoka, A.P., 2025. Effects of prenatal lead, mercury, cadmium, and arsenic exposure on children's neurodevelopment in an artisanal small-scale gold mining area in Northwestern Tanzania using a multi-chemical exposure model. PLOS Glob. Public Health 5, e0004577. https://doi.org/10.1371/journal.pgph.0004577.
Obrist, D., Johnson, D.W., Edmonds, R.L., 2012. Effects of vegetation type on mercury concentrations and pools in two adjacent coniferous and deciduous forests. J. Plant Nutr. Soil Sci. 175, 68–77. https://doi.org/10.1002/jpln.201000415.
Obrist, D., Kirk, J.L., Zhang, L., Sunderland, E.M., Jiskra, M., Selin, N.E., 2018. A review of global environmental mercury processes in response to human and natural perturbations: changes of emissions, climate, and land use. Ambio 47, 116–140. https://doi.org/10.1007/s13280-017-1004-9.
Ogden, J., 1978. Investigations of the dendrochronology of the genus athrotaxis D. Don (Taxodiaceae) in Tasmania.
Paranjape, A.R., Hall, B.D., 2017. Recent advances in the study of mercury methylation in aquatic systems. FACETS 2, 85–119. https://doi.org/10.1139/facets-2016-0027.
Paull, R., 1963. Old Walhalla. Portrait of a Gold Town. Melbourne University Press, Melbourne., Melbourne, VIC, Australia.
Pearson, S., Hua, Q., Allen, K., Bowman, D.M.J.S., 2011. Validating putatively cross-dated Callitris tree-ring chronologies using bomb-pulse radiocarbon analysis. Aust. J. Bot. 59, 7–17. https://doi.org/10.1071/BT10164.
Phillips, G.N., Hughes, M.J., Arne, D.C., Bierlein, F.P., Carey, S.P., Jackson, T., Willman, C.E., 2003. Gold: historical wealth, future potential. In: Birch, W.D. (Ed.), 'Geology of Victoria'. Geological Society of Australia Special Publication 23, Geological Society of Australia (Victoria Division), pp. 377–433.
R Core Team, 2025. R: a Language and Environment for Statistical Computing. R Foundation for Statistical Computing, Vienna, Austria.
Reeves, J.M., Gell, P.A., Reichman, S.M., Trewarn, A.J., Zawadzki, A., 2015. Industrial past, urban future: using palaeo-studies to determine the industrial legacy of the Barwon Estuary, Victoria, Australia. Mar. Freshw. Res. 67, 837–849. https://doi.org/10.1071/MF15344.
Reimer, P.J., Brown, T.A., Reimer, R.W., 2004. Discussion: Reporting and Calibration of Post-bomb 14C Data. UCRL-JRNL-207168.
Reuben, A., Frischtak, H., Berky, A., Ortiz, E.J., Morales, A.M., Hsu-Kim, H., Pendergast, L.L., Pan, W.K., 2020. Elevated hair Mercury levels are associated with neurodevelopmental deficits in children living near artisanal and small-scale gold mining in Peru. GeoHealth 4. https://doi.org/10.1029/2019gh000222 n/a-n/a.
Schneider, L., Allen, K., Walker, M., Morgan, C., Haberle, S., 2019. Using tree rings to track atmospheric Mercury pollution in Australia: the legacy of mining in Tasmania. Environ. Sci. Technol. 53, 5697–5706. https://doi.org/10.1021/acs.est.8b06712.
Schneider, L., Guerrero, S., 2024. From chemistry to culture: the need for an integrated approach to mercury research and policy making. Environ. Chem. 21. https://doi.org/10.1071/EN24096. NULL-NULL.
Schneider, L., Rose, N.L., Myllyvirta, L., Haberle, S., Lintern, A., Yuan, J., Sinclair, D., Holley, C., Zawadzki, A., Sun, R., 2021. Mercury atmospheric emission, deposition and isotopic fingerprinting from major coal-fired power plants in Australia: insights from palaeo-environmental analysis from sediment cores. Environ. Pollut. 287, 117596. https://doi.org/10.1016/j.envpol.2021.117596.
Schweingruber, F.H., 1992. Annual growth rings and growth zones in woody plants in Southern Australia. https://doi.org/10.1163/22941932-90001290.
Singer, M.B., Aalto, R., James, L.A., Kilham, N.E., Higson, J.L., Ghoshal, S., 2013. Enduring legacy of a toxic fan via episodic redistribution of California gold mining debris. Proc. Natl. Acad. Sci. U. S. A 110, 18436. https://doi.org/10.1073/pnas.1302295110.
Siwik, E.I.H., Campbell, L.M., Mierle, G., 2010. Distribution and trends of mercury in deciduous tree cores. Environ. Pollut., Advances of air pollution science: from forest decline to multiple-stress effects on forest ecosystem services 158, 2067–2073. https://doi.org/10.1016/j.envpol.2010.03.002.
SKM, 2006. Stringers Creek Streamscape Plan Implementation. Sinclair Knight Mertz, Melbourne, VIC, Australia.
Stuiver, M., Polach, H.A., 1977. Reporting of 14C data. Radiocarbon 19, 353–363.
Swift, D., Marcuse, H., 1951. The Golden Century. A Brief Story of One Hundred Years of Gold Mining, vol. 4, pp. 5–17.
Taylor, J.R., Schneider, L., Fostier, A.-H., Keith, H., Cao, F., Davies, P., Cary, G.J., Haberle, S.G., Lawrence, S., 2025. Mercury in an Australian sclerophyll Eucalyptus forest and emissions from fuel reduction prescribed burning. Environ. Chem. 22. https://doi.org/10.1071/EN24087.
Trewin, 2018. The Australian Climate Observation Reference Network - Surface Air Temperature (ACORN-SAT) Version 2. Bureau of Meteorology Research Report No. 032.
Tshering, C., Tenzin, K., Nguyen, T.V., 2023. A review of the Current State and future prospects of dendrochronological research in Bhutan. Tree-Ring Res. 79, 41–49. https://doi.org/10.3959/2022-6.
UNEP, 2025. Australia | Minamata Convention on Mercury [WWW Document]. URL. https://minamataconvention.org/en/parties/aus, 4.24.25.
UNEP/MAP, 2019. IMAP Monitoring Guidelines: Common Indicator 17 – Concentration of Key Harmful Contaminants Measured in the Relevant Matrix (Biota, Sediment, Seawater). United Nations Environment Programme/Mediterranean Action Plan, Athens, Greece.
USEPA, 1998. Method 7473 - Mercury in Solids and Solutions by Thermal Decomposition, Amalgamation, and Atomic Absorption Spectrophotometry (No. SW-846-). US Environmental Protection Agency, Washington, D.C.
Victoria 1852–1901, 1852. Statistical Register of Victoria. Parliament of Victoria, Melbourne, Australia.
Victoria Department of Mines, 1890. Mineral Statistics of Victoria. Mines Department, Melbourne, pp. 1868–1890. Years.
Victorian Government, 2016. Victorian Soil Type Mapping.
Wang, Q., Li, Y., Wang, Y., 2011. Optimizing the weight loss-on-ignition methodology to quantify organic and carbonate carbon of sediments from diverse sources. Environ. Monit. Assess. 174, 241–257. https://doi.org/10.1007/s10661-010-1454-z.
Watson, E., Luckman, B.H., 2002. The dendroclimatic signal in Douglas-fir and ponderosa pine tree-ring chronologies from the southern Canadian Cordillera. Can. J. For. Res. 32, 1858–1874. https://doi.org/10.1139/x02-096.
Wickham, H., Chang, W., Henry, L., Pedersen, T.L., Takahashi, K., Wilke, C., Woo, K., Yutani, H., Dunnington, D., 2024. ggplot2: Create Elegant Data Visualisations Using the Grammar of Graphics. R package version 4.0.1.
Wilcken, K.M., Hotchkis, M., Levchenko, V., Fink, D., Hauser, T., Kitchen, R., 2015. From carbon to actinides: a new universal 1MV accelerator mass spectrometer at ANSTO. Nucl. Instrum. Methods Phys. Res. Sect. B Beam Interact. Mater. At., The Thirteenth Accelerator Mass Spectrometry Conference 361, 133–138. https://doi.org/10.1016/j.nimb.2015.04.054.
Witt, G.B., English, N.B., Balanzategui, D., Hua, Q., Gadd, P., Heijnis, H., Bird, M.I., 2017. The climate reconstruction potential of *Acacia cambagei* (gidgee) for semi-arid regions of Australia using stable isotopes and elemental abundances. J. Arid Environ. 136, 19–27. https://doi.org/10.1016/j.jaridenv.2016.10.002.
Wright, G., Woodward, C., Peri, L., Weisberg, P.J., Gustin, M.S., 2014. Application of tree rings [dendrochemistry] for detecting historical trends in air Hg concentrations across multiple scales. Biogeochemistry 120, 149–162. https://doi.org/10.1007/s10533-014-9987-9.